Consensus chemistry and β-turn conformation of the active core of the insect kinin neuropeptide family

Victoria A Roberts[1], Ronald J Nachman[2], Geoff M Coast[3], Meena Hariharan[1]*, Jum S Chung[3], G Mark Holman[2], Howard Williams[4] and John A Tainer[1]

Background: Neuropeptides are examples of small, flexible molecules that bind to receptors and induce signal transduction, thereby eliciting biological activity. The multifunctional insect kinin neuropeptides retain full activity when reduced to only their carboxy-terminal pentapeptide (Phe^1–X^2–X^3–Trp^4–Gly^5–NH_2), thereby allowing extensive structure–function studies and conformational analysis.

Results: A combined experimental and theoretical analysis of the insect kinin carboxy-terminal pentapeptide was used to probe the role of each residue, define the bioactive conformation, and design a constrained bioactive analog. Coupling receptor-binding data with two biological activity assays allowed receptor binding and signal transduction to be differentiated. A preferred β-turn conformation, found for residues 1–4 by molecular dynamics simulations, was tested by designing a conformationally restricted cyclic hexapeptide. This cyclic analog showed a preference for the β-turn conformation, as shown by a conformational search and nuclear magnetic resonance spectroscopy, and it showed stronger receptor binding but decreased activity relative to highly active linear analogs.

Conclusions: Each residue of the insect kinin carboxy-terminal pentapeptide has a distinct role in conformational preference, specific receptor interactions or signal transduction. The β-turn preference of residues Phe^1–X^2–X^3–Trp^4 implicates this as the bioactive conformation. The amidated carboxyl terminus, required for activity in many neuropeptide families, may be generally important for signal transduction and its inclusion may therefore be essential for agonist design.

Addresses: [1]Department of Molecular Biology, The Scripps Research Institute, La Jolla, CA 92037, USA, [2]Veterinary Toxicology and Entomology Research Laboratory, US Department of Agriculture, College Station, TX 77845, USA, [3]Department of Biology, Birkbeck College, University of London, Malet St., London WC1E 7HX, UK and [4]Department of Chemistry, Texas A & M University, College Station, TX 77843, USA.

Present address: *Department of Biochemistry, University of Minnesota, 1479 Gortner Ave, Saint Paul, MN 55114, USA.

Correspondence: Victoria A Roberts
E-mail: vickie@scripps.edu

Key words: *cis* proline, molecular dynamics, nuclear magnetic resonance, receptor binding, signal transduction

Received: **18 September 1995**
Revisions requested: **5 October 1995**
Revisions received: **2 January 1997**
Accepted: **17 January 1997**

Electronic identifier: **1074-5521-004-00105**

Chemistry & Biology February 1997, 4:105–117

Introduction

A single neuropeptide can interact with multiple receptors, resulting in multiple biological activities. Well-known examples include the opioid [1] and tachykinin [2] neuropeptides. If a neuropeptide binds with a distinct conformation to each receptor, it should be possible to develop receptor-selective ligands that would not interfere with functions of the neuropeptide mediated by any other receptor [3]. Determining the conformation of the receptor-bound peptide would greatly aid the design of selective ligands. Protein X-ray crystallography is the best way to determine the structure of bound ligands, but, due to difficulties in their expression, isolation and crystallization, few receptor proteins are amenable to this method. Instead, receptor-binding properties are usually inferred from structural analysis of ligands and ligand analogs [4], but, because of the flexibility of peptides, the receptor-bound conformation may not resemble the peptide structure in solution or in the crystal. Combining activity data from related neuropeptides and their analogs with determination of shared conformational preferences, however, provides a rational basis for probing receptor structure and designing conformationally restricted agonists and antagonists. Characterization of these designed analogs then provides further information on structural requirements for receptor binding and signal transduction.

Because the insect kinin neuropeptide family [5–9] consists of many naturally occurring homologs of short amino-acid sequence (typically 6–9 residues), it is well-suited for a synthesis of experimental and theoretical approaches to elucidate stereochemical requirements for activity. Members of this family have been isolated from such diverse sources as the cockroach *Leucophaea*, the cricket *Acheta*, the locust *Locusta*, and the mosquitoes *Culex* and *Aedes*. The leucokinin members of the family are myotropic (muscle-contracting) octapeptides of the Madeira cockroach, *Leucophaea maderae*, isolated from extracts of the corpora cardiaca [5], the major neurohumoral organ in insect brains (analogous to the vertebrate hypothalamo–hypophyseal system). The related achetakinin peptides are obtained from head extracts of the cricket, *Acheta domesticus*, and stimulate Malpighian tubule fluid secretion in this species [10]. Some leucokinins also show diuretic activity (stimulating fluid secretion and/or depolarizing transepithelial membrane potentials) in the Malpighian tubules of the yellow fever mosquito, *Aedes aegypti* [11].

The cross-reactivity displayed by the neuropeptide family of leucokinins, achetakinins and homologs among receptors from three species of insects — cockroaches, crickets and mosquitoes — implicates these peptides in multiple functions, including myotropic activity and the control of water and ion balance. Myotropic activity can be determined by a rapid and reproducible bioassay in which the contractile activity of isolated cockroach proctodeum (hindgut) is measured. Full myotropic activity of the insect kinins is retained in their carboxy-terminal pentapeptide — Phe^1–X^2–Ser^3–Trp^4–Gly^5–NH_2 (X = Tyr, His, Asn or Ser) for the leucokinins and Phe^1–X^2–Pro^3–Trp^4–Gly^5–NH_2 (X = Tyr, Ser and Asn) for the achetakinins — and requires very low threshold neuropeptide concentrations (10^{-10}– 10^{-11} M) [6,10]. Phe^1 and Trp^4 are essential for myotropic activity [6]. A second probe for biological activity of the leucokinins and the achetakinins is the measurement of increased diuretic activity on Malpighian tubules of crickets [10], which takes place at neuropeptide concentrations of about 10^{-10} M.

In this paper, we show that leucokinin and achetakinin analogs have similar activity profiles in the myotropic and the diuretic assays, suggesting that the diuretic and myotropic receptors recognize closely related conformations of the peptides. Myotropic activity is more sensitive to substitutions of Gly^5, however, providing the potential for selective analog design. Conformational search by distance geometry and molecular dynamics methods revealed that the carboxy-terminal active-core pentapeptides from both families of neuropeptides have a shared conformational preference. A cyclic hexapeptide designed to maintain this preferred conformation showed significant, but reduced, biological activity in both myotropic and diuretic assays when compared with highly active linear analogs. The cyclic hexapeptide, however, bound more tightly to the diuretic receptor than linear analogs, suggesting that reduced message transmission, rather than reduced receptor binding, was responsible for the decreased activity. Thus, the amidated carboxyl terminus, which occurs in many insect and mammalian neuropeptides but is lacking in the cyclic analog, may be crucial for signal transduction.

Results

The leucokinin active core is Phe^1–X^2–Ser^3–Trp^4–Gly^5–NH_2 and the achetakinin active core is Phe^1–X^2–Pro^3–Trp^4–Gly^5–NH_2. Leucokinin peptide fragments will be referred to as LPF and achetakinin peptide fragments as APF. Analogs of LPF or APF will be defined by indicating the residue in variable position 2 and any changes in the active core. For example, LPF[Tyr^2,Ala^5] is the leucokinin active core analog with Tyr in position 2 and active-core residue Gly^5 replaced by Ala. Each peptide has an amidated carboxyl terminus unless explicitly indicated.

Effects of Ala substitution on the diuretic activity of the active core of the leucokinins

Analogs with a single Ala substitution at each of the five positions of the leucokinin active core were evaluated

Table 1

Diuretic activities of leucokinin fragments/analogs on isolated Malpighian tubules of the cricket.

Peptide	Peptide sequence	EC_{50}*($\times 10^{-10}$ M)
LPF[Tyr^2]†	**Phe** – Tyr – **Ser** – **Trp** – **Gly** – **NH_2**	0.1
LPF[Ala^1,Tyr^2]	**Ala** – Tyr – Ser – Trp – Gly – NH_2	inactive‡
LPF[Ala^2]	Phe – **Ala** – Ser – Trp – Gly – NH_2	2.5
LPF[Tyr^2,Ala^3]	Phe – Tyr – **Ala** – Trp – Gly – NH_2	1.3
LPF[Tyr^2,Ala^4]	Phe – Tyr – Ser – **Ala** – Gly – NH_2	inactive‡
LPF[Tyr^2,Ala^5]	Phe – Tyr – Ser – Trp – **Ala** – NH_2	0.9
LPF[DAla^2]	Phe –**DAla**– Ser – Trp – Gly – NH_2	inactive‡
LPF[Phe^2,Asn^5]	Phe – Phe– Ser – Trp – **Asn**– NH_2	360
LPF[Phe^2,Leu^5]	Phe – Phe– Ser – Trp – **Leu**– NH_2	580
APF[Tyr^2]†	**Phe** – Tyr – **Pro** – **Trp** – **Gly** – **NH_2**	0.55
APF[Phe^2]	Phe – **Phe**– Pro – Trp – Gly – NH_2	1.0
APF[Ser^2]	Phe – **Ser**– Pro – Trp – Gly – NH_2	3.0
LPF[Ala^0,Phe^2]	**Ala** – Phe – Phe– Ser– Trp – Gly – NH_2	0.04
APF[Ala^0,Phe^2]	**Ala** – Phe – Phe– Pro – Trp – Gly – NH_2	0.2
APF[Ala^0,Phe^2]–OH	**Ala** – Phe – Phe– Pro – Trp – Gly – **OH**	10000
APF[Phe^2,Ala^6]	Phe – Phe– Pro – Trp – Gly – **Ala** – **NH_2**	4.0#
APF[Phe^2,Ala^6]–OH	Phe – Phe– Pro – Trp – Gly – **Ala** – **OH**	600
cyclo-(APF[Phe^2,Ala^6])	cyclo-(Phe – Phe– Pro – Trp – Gly – Ala)	30.0#

Abbreviations: LPF = leucokinin pentapeptide fragment (Phe–X–Ser–Trp–Gly–NH_2), APF = achetakinin pentapeptide fragment (Phe–X–Pro–Trp–Gly–NH_2). The conserved active core residues are highlighted for leucokinins and achetakinins. In analogs, replacements in the active core are highlighted. *Effective concentration for 50% activity. †See [10]. ‡Inactive at concentrations up to 1×10^{-6} M. #Difference is not statistically significant. When tested at 10^{-9} M, the point at which the dose-response curves of APF[Phe^2,Ala^6] and cyclo(APF[Phe^2,Ala^6]) diverge (Fig. 4), no statistically significant difference in activity could be observed in the diuretic assay.

Table 2

Myotropic activities of the leucokinin fragments/analogs on isolated cockroach hindgut.

Peptide	Peptide sequence	Threshold concentration* ($\times 10^{-10}$M)
Leucokinin-VIII†	Gly – Ala – Asp – **Phe** – Tyr – **Ser** – **Trp** – **Gly** – **NH_2**	0.3 ± 0.05
Leucokinin-II†	Asp – Pro – Gly – **Phe** – Ser – **Ser** – **Trp** – **Gly** – **NH_2**	2.0 ± 0.4
LPF[Tyr^2]†	**Phe** – Tyr – **Ser** – **Trp** – **Gly** – **NH_2**	0.2 ± 0.06
LPF[Phe^2]†	Phe – **Phe** – Ser – Trp – Gly – NH_2	0.2 ± 0.08
LPF[Ser^2]†	Phe – **Ser** – Ser – Trp – Gly – NH_2	2.0 ± 0.5
LPF[Tyr^2]–OH†	Phe – Tyr – Ser – Trp – Gly – **OH**	inactive‡
LPF[Ala^1,Tyr^2]†	**Ala** – Tyr – Ser – Trp – Gly – NH_2	inactive‡
LPF[Ala^2]†	Phe – **Ala** – Ser – Trp – Gly – NH_2	8 ± 1.9
LPF[Tyr^2,Ala^3]†	Phe – Tyr – **Ala** – Trp – Gly – NH_2	0.4 ± 0.1
LPF[Tyr^2,Ala^4]†	Phe – Tyr – Ser – **Ala** – Gly – NH_2	inactive‡
LPF[Tyr^2,Ala^5]†	Phe – Tyr – Ser – Trp – **Ala** – NH_2	6 ± 0.9
LPF[DAla^2]†	Phe –**DAla**– Ser – Trp – Gly – NH_2	inactive#
LPF[Phe^2,Asn^5]	Phe – Phe – Ser – Trp – **Asn**– NH_2	680 ± 240
LPF[Phe^2,Leu^5]	Phe – Phe – Ser – Trp – **Leu** – NH_2	12000 ± 3000
Achetakinin–I†	Ser – Gly – Ala – Asp – **Phe** – Tyr – **Pro** – **Trp** – **Gly** – **NH_2**	0.9 ± 0.5
APF[Tyr^2]†	**Phe** – Tyr – **Pro** – **Trp** – **Gly** – **NH_2**	0.4 ± 0.06
APF[Ala^0,Phe^2]	**Ala** – Phe – Phe – Pro – Trp – Gly – NH_2	0.07 ± 0.01
APF[Phe^2,Ala^6]	Phe – Phe – Pro – Trp – Gly – **Ala** – **NH_2**	170 ± 20
APF[Phe^2,Ala^6]–OH	Phe – Phe – Pro – Trp – Gly – **Ala** – **OH**	12000 ± 3,000
cyclo-(APF[Phe^2,Ala^6])	cyclo-(Phe – Phe – Pro – Trp – Gly – Ala)	650 ± 250

Abbreviations and highlighting as in Table 1. *Average of five replicates. Procedure for threshold concentration determinations described previously [5]. †See [6]. ‡Inactive up to at least 1×10^{-6}M. #Inactive up to at least 1×10^{-5}M.

in a diuretic assay (Table 1) and a myotropic assay (most of the myotropic data come from a previous study [6]) (Table 2). Loss of activity upon substitution of the aromatic side chains at positions 1 or 4 demonstrates the requirement for active-core residues Phe^1 and Trp^4 in both diuretic and myotropic activities. At concentrations of 10^{-6}–10^{-7}M, the leucokinin peptide fragment with Ala^1 and Tyr^2 (LPF[Ala^1,Tyr^2]) inhibited the diuretic activity of the achetakinins present at 10^{-9}M (data not shown). This analog demonstrated receptor binding (Table 3). As in the myotropic assay [6], substitution of D-Ala at position 2, LPF[DAla^2], resulted in loss of activity in the diuretic assay.

Conformational analysis of leucokinins, achetakinins and linear analogs

The high activity of achetakinin APF[Tyr^2] in both the diuretic and myotropic assays showed that the leucokinin active-core residue Ser^3 can be replaced by Pro. This suggests that the leucokinins and achetakinins share similar active conformations. To investigate the conformational preferences of these peptides, molecular dynamics simulations were carried out. The simulations were started from energy-minimized extended structures. Between 40 and 50 picoseconds (ps) into the dynamics simulation of the leucokinin L-II (Asp–Pro–Gly–Phe–Ser–Ser–Trp–Gly–NH_2, Table 2), the first four residues of the carboxy-terminal active core (Phe–Ser–Ser–Trp) folded into a β-turn conformation, thus allowing the Phe and Trp sidechains to come close together, while the three non-essential amino-terminal residues remained extended. This folded conformation was maintained for the rest of the simulation (total of 100 ps). During the 100 ps molecular dynamics simulations, three naturally occurring active-core leucokinin sequences (X^2 = Tyr, Ser or Asn) folded into a similar β-turn conformation, again with the aromatic Phe^1 and Trp^4 sidechains coming close together.

Table 3

Thermodynamic dissociation constants (K_i) of insect kinin analogs to the diuretic receptor.

Peptide	Peptide sequence	K_i (μM)
APF[Ala^0,Phe^2]	Ala – Phe – Phe – Pro – Trp – Gly – NH_2	2.5
APF[Ala^0,Phe^2]–OH	Ala – Phe – Phe – Pro – Trp – Gly – OH	4.9
APF[Phe^2,Ala^6]	Phe – Phe – Pro – Trp – Gly – Ala – NH_2	6.45
cyclo-(APF[Phe^2,Ala^6])	cyclo-(Phe – Phe – Pro – Trp – Gly – Ala)	0.129
LPF[Ala^1,Tyr^2]	Ala – Tyr – Ser – Trp – Gly – NH_2	1.77

LPF[His^2] retained the starting extended conformation throughout the 100 ps of dynamics, probably due to favorable interactions between the aromatic sidechains of His^2 and Trp^4. Rather than continue the simulation, LPF[His^2] was fitted onto the β-turn conformation of LPF[Tyr^2] by forcing the Cα atoms of LPF[His^2] onto a template formed by the corresponding Cα atoms of LPF[Tyr^2] (see the Materials and methods section). Subsequent unconstrained energy minimization gave a conformation with an intramolecular energy about 15 kcal mol^{-1} more favorable than that of the extended conformation. This conformation, which closely resembled the β-turn conformation of LPF[Tyr^2], was still retained during an additional 50 ps of unconstrained molecular dynamics.

Two snapshots taken from the dynamics trajectories of LPF[Ser^2] and LPF[Tyr^2] (Fig. 1) are typical of the low-energy conformations found for the leucokinin active core. Backbone and sidechain placements are very similar, despite differences in β-turn type (type I for LPF[Ser^2] and type II for LPF[Tyr^2]). The sidechain in position 2 of the active-core pentapeptide extends away from the molecule, consistent with the sequential diversity found for this position in both leucokinins and achetakinins and with the extensive variation allowed in position 2 of the leucokinin active core [6]. The essential Phe^1 and Trp^4 sidechains are on the same side of the peptide backbone, forming a surface that might be involved in the interaction with the receptor. The close proximity of these two sidechains may therefore be important for biological activity.

Figure 1

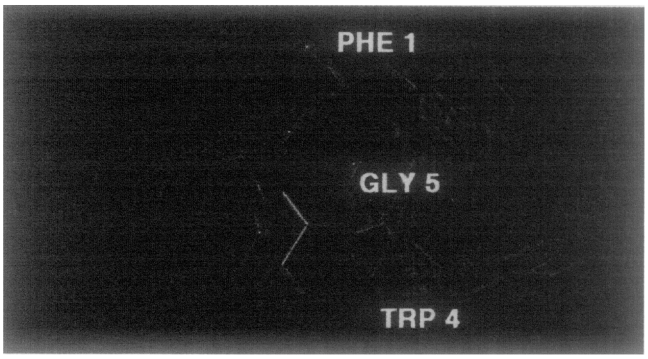

Preferred conformations of insect kinin linear active-core peptides. The conformations found by molecular dynamics simulation for the leucokinin active cores LPF[Tyr^2] (orange, energy-minimized conformation after 100 ps of dynamics) and LPF[Ser^2] (purple, energy-minimized after 50 ps of dynamics) have a β-turn for residues 1–4. Template forcing of the achetakinin active core APF[Tyr^2] (colored by atom type, C=green, N=blue, O=red) to LPF[Tyr^2] followed by energy minimization provided a similar conformation in which Pro^3 is preceded by a *cis* peptide bond. In all three structures, the sequence-variable position 2 sidechain lies on one side of the backbone and the Phe^1 and Trp^4 sidechains lie near each other on the other side of the peptide backbone.

To investigate whether the achetakinins could adopt this conformation, the Cα atoms of APF[Tyr^2] were forced onto the template formed by the corresponding atoms of the folded LPK[Tyr^2] conformation. These constraints caused the peptide bond between Tyr^2 and Pro^3 to rotate, creating a type VI β-turn with Pro^3 in the third (i+2) position preceded by a *cis* peptide bond (*cis* Pro). Refinement of the conformation by unconstrained minimization gave an APF[Tyr^2] structure with a type VIA β-turn ($\phi_2 = -139°$, $\psi_2 = 109°$, $\phi_3 = -44°$ and $\psi_3 = -47°$) having approximately α-helical torsion angles for the Pro residue. This conformation, which was retained during an additional 50 ps of unconstrained molecular dynamics, displayed the overall structural features found for low-energy conformations of LPK[Tyr^2] and LPK[Ser^2] (Fig. 1), including the close proximity of the Phe^1 and Trp^4 sidechains.

Due to the common occurrence of *trans* Pro in position 2 (i+1) of β-turns in proteins, calculations based on parameters from protein sequence analysis [12,13] showed that residues 2–5 of the achetakinin active core preferred a β-turn conformation. To examine the conformational preference of APF[Tyr^2] with *trans* Pro, this structure was subjected to 50 ps of molecular dynamics with snapshots taken every 10 ps. The energy-minimized snapshots all contained a type I β-turn for residues 2–5, with Pro in the i+1 position preceded by a *trans* peptide bond. The corresponding β-turn conformation for the linear leucokinin active cores was not observed in the molecular dynamics simulations. Forcing the Cα and Cβ atoms of LPF[Tyr^2] onto a template of the lowest-energy conformation of *trans* Pro APF[Tyr^2] showed that LPF[Tyr^2] could adopt this type of β-turn structure. Subsequent unconstrained minimization, however, resulted in the formation of an additional β-turn for residues 1–4, bringing together the Phe^1 and Trp^4 sidechains.

Sensitivity of the amino terminus and carboxyl terminus to modification

In the preferred conformations found for the leucokinins and the achetakinins (with both *cis* and *trans* Pro) the amino-terminus and carboxyl terminus were positioned near each other. This suggests that the cyclic analogs of the active core could be active. Peptide cyclization methods, such as the formation of a disulfide bond and end-to-end cyclization to form a cyclic peptide backbone, require modification of the amino-terminal and carboxy-terminal residues. The natural variation of the sidechain preceding the kinin active core indicates that amino-terminal modifications are well tolerated. Addition of an Ala residue before the achetakinin active core (APF[Ala^0,Phe^2]) showed improved activity in both assays (Tables 1 and 2). Replacement of carboxy-terminal Gly^5 by Ala in the leucokinin active core (LPF[Tyr^2,Ala^5]), however, decreased activity, especially in the myotropic assay (30-fold increase in threshold concentration,

Table 2). Replacement of the carboxy-terminal amide by the free acid was more deleterious in both assays (Tables 1 and 2). Replacing Gly^5 by Asn or Leu, LPF[Phe^2,Asn^5] and LPF[Phe^2,Leu^5], caused large reductions in activity (Tables 1 and 2) with myotropic activity being more adversely affected than diuretic activity.

APF[Phe^2,Ala^6], a permuted analog of the highly active APF[Ala^0,Phe^2] that retains the active core but has Ala^6 inserted between Gly^5 and the carboxy-terminal amide, showed the effect of adding residues at the carboxyl terminus. In the diuretic assay, APF[Phe^2,Ala^6] still displayed about 25% of the activity of the pentapeptide APF[Phe^2] (Table 1), whereas in the myotropic assay, the carboxy-terminal elongation caused a larger decrease in activity (Table 2), consistent with myotropic activity having stricter requirements at the carboxyl terminus.

Characterization of a cyclic disulfide analog

The disulfide cyclo[Cys–Phe–Tyr–Ser–Trp–Cys–NH_2], in which Gly^5 is replaced with Cys, had measurable, but low, myotropic activity [6]. The corresponding linear analog was only slightly more active, having one third the threshold concentration of the disulfide. The results from the Asn^5 and Leu^5 analogs suggest that the steric bulk of Cys^5 causes the decreased activities; alternatively, free Cys residues may destabilize the peptide under the assay conditions or the conformationally constrained disulfide analog may be unable to adopt the biologically active conformation. The flexibility of the cyclic disulfide was examined with molecular dynamics simulations starting from a conformation based on the β-turn structure of LPF[Tyr^2]. The cyclic disulfide demonstrated substantial conformational freedom, readily adopting the conformation common to the linear leucokinins and achetakinins. Thus, the low activity of the disulfide does not appear to be due to conformational restrictions.

An end-to-end cyclized analog

Retention of biological activity in amino-terminal and carboxy-terminal analogs indicated that an end-to-end cyclized peptide could be active, especially in the diuretic assay. The conformational space of the cyclic achetakinin analog cyclo[Phe–Phe–Pro–Trp–Gly–Ala] — or cyclo-(APF[Phe^2,Ala^6]) for short — was explored with molecular dynamics. Two structures, one with *cis* and one with *trans* Pro, were constructed by computer graphics (see the Materials and methods section). An additional five starting structures each for both *cis* and *trans* Pro were generated with distance geometry methods in which the Ala^6 carbonyl was constrained to be near the Phe^1 amino group. The starting structures showed substantial structural variation (Fig. 2). All structures were relaxed by energy minimization followed by 100 ps of molecular dynamics. Dynamics snapshots were taken every 10 ps and energy minimized, resulting in 66 structures each for *cis* and *trans* cyclo-(APF[Phe^2,Ala^6]). The most favorable *cis* Pro structure had an intramolecular energy about 7 kcal mol^{-1} lower than the most favorable *trans* Pro structure, suggesting that the *cis* conformation should predominate. In each trajectory, there was an equilibration period of 10–50 ps corresponding to a large drop in internal potential energy. This was followed by a further 50–90 ps in which there was little conformational change and a constant potential energy. After equilibration, the root mean square (rms) deviations between the Cα atoms for the minimized snapshots, obtained from any given trajectory, were 0.3 Å or less.

The low-energy *cis* and *trans* Pro cyclic peptide structures contained the β-turn types found for the corresponding conformations of the achetakinin linear active core. The lowest-energy *cis* Pro conformation was obtained from the structure built by computer graphics. Trajectories starting from two of the structures generated by distance geometry provided conformations within 5 kcal mol^{-1} of the lowest-energy structure. All three low-energy structures resembled the linear *cis* Pro structure, displaying a type VIA β-turn for residues Phe–Phe–Pro–Trp ($\phi_2 \approx -75°$, $\psi_2 \approx 135°$, $\phi_3 \approx -80°$, $\psi_3 \approx -5°$), a Cβ-*exo*/Cγ-*endo* Pro-ring pucker (χ_1) of about 30° and close approach of the essential Phe^1 and Trp^4 sidechains on the same side of the peptide backbone (Fig. 3a).

The lowest-energy *trans* Pro conformation was obtained from a structure generated by distance geometry.

Figure 2

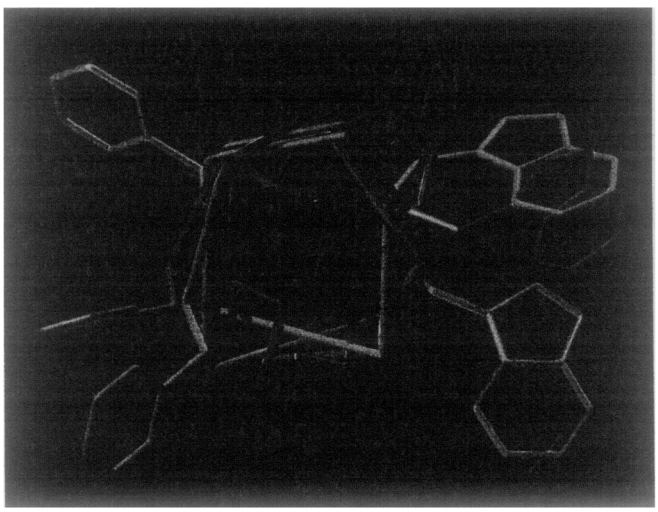

Variation in the starting conformations of cyclo-(APF[Phe^2,Ala^6]) with a *cis* Pro geometry. The Cα backbone and Phe^1 and Trp^4 sidechains are shown. The five conformations built by distance geometry methods are superimposed by their Cα atoms onto the conformation built by computer graphics (red). The two most similar structures (red and green) were constructed by different methods.

Trajectories starting from the structure that was built by computer graphics and three additional structures generated by distance geometry gave conformations within 5 kcal mol^{-1} of the lowest energy structure (Fig. 3b). Four structures displayed a type I β-turn for residues 2–5 ($\phi_3 \approx -55°$, $\psi_3 \approx -30°$, $\phi_4 \approx -100°$ and $\psi_4 = 16–80°$) (Fig. 3b) and one displayed an approximate type II β-turn for residues 2–5 ($\phi_3 \approx -82°$, $\psi_3 \approx 78°$, $\phi_4 \approx 72°$ and $\psi_4 \approx -54°$). Both the Cβ-*exo*/C^{γ}-*endo* (χ_1 about 30°) and Cβ-*endo*/C^{γ}-*exo* (χ_1 about −30°) Pro-ring puckers were present. In the low-energy *trans* Pro structures, the Phe^1 and Trp^4 sidechains were distant from each other on opposite sides of the peptide backbone structure (Fig. 3b), a very different arrangement than that found for the linear kinin active core (Fig. 1). The internal potential energy of the most favorable *trans* Pro structure was 7 kcal mol^{-1} higher than that of the most favorable *cis* Pro structure.

Biological activity and receptor binding of cyclo-(APF[Phe^2, Ala^6])

The biological activity of cyclo-(APF[Phe^2, Ala^6]) was comparable to the corresponding permuted linear peptide APF[Phe^2, Ala^6] in both the diuretic (Table 1, Fig. 4) and myotropic (Table 2) assays. This cyclic analog was much more active than APF[Phe^2, Ala^6]–OH (Fig. 4) and APF[Ala^0, Phe^2]–OH in the diuretic assay (Table 1) and APF[Phe^2, Ala^6]–OH in the myotropic assay (Table 2), thus showing that the two possible hydrolysis products with an intact active core were not responsible for the activity of cyclo-(APF[Phe^2, Ala^6]).

Figure 3

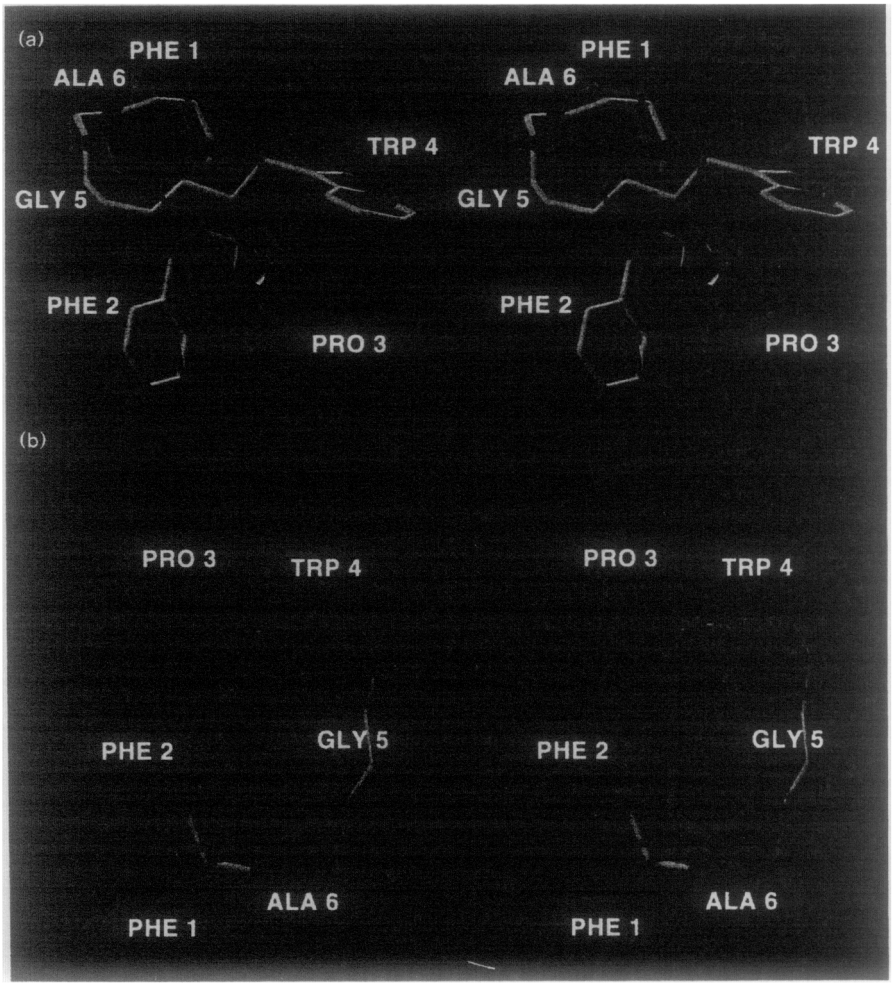

Low-energy conformations of cyclo[Phe–Phe–Pro–Trp–Gly–Ala] found by computational search. **(a)** Low-energy *cis* Pro structures. In all structures, the Phe^1 and Trp^4 sidechains lie near each other on one side of the ring formed by the cyclic mainchain, and the sequence variable position 2 sidechain lies on the opposite side of the ring, extending away from the surface formed by the two essential sidechains. The lowest energy structure (colored by atom type, C=green, N=blue, O=red) was obtained from the simulation starting with the structure built by computer graphics. The two structures (pink and yellow mainchain atoms displayed with Phe^2 and Trp^4 sidechains) have energies within 5 kcal mol^{-1} of the lowest energy structure and were obtained from simulations starting with structures generated by distance geometry methods. **(b)** Low energy *trans* Pro structures. The lowest energy structure (colored by atom type) was obtained from a simulation starting with a conformation generated by distance geometry and has a type I β-turn for residues Phe^2 to Gly^5. Three additional structures (orange, yellow, and purple mainchain atoms displayed) have energies within 5 kcal mol^{-1} of the lowest energy structure and have a type I β-turn. Two (yellow and purple mainchain tubes) are from simulations starting with conformations generated by distance geometry and one (orange mainchain tube) is from the simulation starting with the conformation built using computer graphics. The orange structure, from the simulation starting with a structure built by computer graphics, and the yellow structure have almost identical mainchain conformations (RMS deviation less than 0.1 Å for all mainchain atoms) despite being based on starting structures generated by different methods. A fifth low-energy structure (pink) has an approximate type II β-turn for residues Phe^2 to Gly^5. In all low-energy *trans* Pro structures, the essential Phe^1 and Trp^4 sidechains are distant from each other.

Figure 4

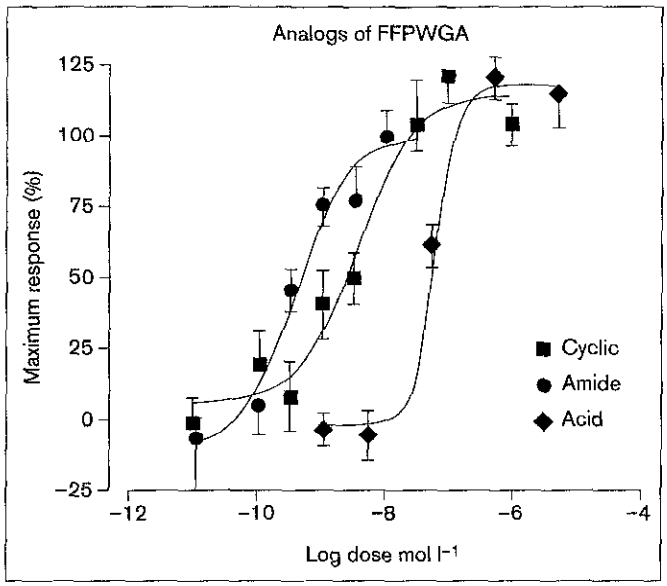

Dose-response curves for analogs of the insect kinin sequence FFPWGA in the cricket Malpighian tubule fluid secretion (diuretic) assay. Depicted are cyclo-(APF[Phe^2, Ala^6]) (■) and the linear analogs APF[Phe^2, Ala^6] (●) and APF[Phe^2, Ala^6]–OH (◆). The points represent the means of 6–12 determinations and the vertical lines represent the standard error. The results are expressed as a percentage of the response to a supramaximal dose (10 nM) of achetakinin I. The curve is fitted to a generalized logistic equation using the computer program FigP (Biosoft, Cambridge, UK) and all points are weighted equally.

Receptor dissociation constants

To investigate whether weak receptor binding was contributing to the decrease of biological activity for cyclo-(APF[Phe^2, Ala^6]), receptor binding was examined directly using competition studies in the diuretic assay. Displacement of a bound, radiolabeled achetakinin ligand (see the Materials and methods section) showed that cyclo-(APF[Phe^2, Ala^6]) bound about 20-fold more tightly than the highly active APF[Ala^0, Phe^2] (Table 3). Two linear analogs with modified carboxy-terminal regions, APF [Ala^0, Phe^2]–OH and APF[Phe^2, Ala^6], displayed receptor binding comparable to that of APF[Ala^0, Phe^2] (Table 3). This was surprising given the very low biological activity of APF[Ala^0, Phe^2]–OH. Thus, these carboxy-terminal modified analogs appear to retain the structural characteristics necessary for receptor binding, suggesting that the decrease in biological activity is due to their decreased signal transduction activity.

NMR structure of cyclo-(APF[Phe^2, Ala^6])

Nuclear magnetic resonance (NMR) spectra of cyclo-(APF[Phe^2,Ala^6]) revealed a 60:40 mixture of *cis* to *trans* Pro conformations in a solvent mixture of 30% CD_3CN/ 70% H_2O (CD_3CN was required to prevent precipitation at room temperature). All mainchain and most sidechain protons for both conformations (Table 4) were assigned using spectra from double-quantum filtered two-dimensional correlated spectroscopy (COSY), total correlated spectroscopy (TOCSY) and rotating-frame nuclear Overhauser effect (NOE) spectroscopy (ROESY). The *cis* Pro isomer has four features characteristic of a type VI β-turn structure [14,15]: a large mole fraction of the *cis* form; an upfield shift for the Pro ring protons; a small coupling constant between the amide and the Cα protons for the residue preceding Pro; and a short distance between the Cα proton of the residue preceding Pro and the amide proton of the residue following Pro. The percentage of *cis* Pro isomer in cyclo-(APF[Phe^2, Ala^6]) was among the

Table 4

Chemical shifts (ppm) for the *cis* and *trans* Pro structures of cyclo-(APF[Phe^2, Ala^6]).

Atom	Residue					
	Phe^1	Phe^2	Pro^3	Trp^4	Gly^5	Ala^6
cis						
NH	7.41	8.33		8.27	7.92	8.45
$C_\alpha H$	4.73	4.78	3.47	4.74	3.58, 4.10	4.03
$C_\beta H$	3.01, 3.25	2.92, 3.18	0.60, 1.49	3.27, 3.39		1.27
$C_\gamma H$			0.30, 1.23			
$C_\delta H$	NA	7.27	2.71, 3.02	7.18		
$N_\varepsilon H$				10.04		
$C_\varepsilon H$	NA	NA		7.68		
trans						
NH	7.36	7.72		6.52	7.54	8.49
$C_\alpha H$	4.41	4.66	4.17	3.98	3.95	3.86
$C_\beta H$	2.66, 2.99	1.91, 2.00	1.88, 2.33	3.34, 3.58		1.29
$C_\gamma H$			2.00, 2.17			
$C_\delta H$	7.11	NA	3.30, 3.78	7.44		
$N_\varepsilon H$				10.07		
$C_\varepsilon H$	NA	NA		7.64		

NA = not assigned.

highest percentages found for related linear peptides [15]. The resonances of the *cis* Pro ring were significantly shifted upfield, by 0.4–1.9 parts per million (ppm), relative to the corresponding resonances in the *trans* Pro structure (Table 4). The amide proton of Phe^2, the residue preceding Pro^3, appeared as a broadened singlet, indicating a small (<3 Hz) coupling constant between the Phe^2 Cα and amide protons. The Phe^1, Phe^2 and Trp^4 Cα protons had very close chemical shift values in the 30% CD_3CN/70% H_2O solvent, causing overlapping NOE peaks (Table 4). In 100% CD_3CN, these three Cα protons displayed distinct chemical shifts in COSY and ROESY spectra revealing a strong NOE connectivity between the Phe^2 Cα and Trp^4 amide protons. In 100% CD_3CN, the *cis* Pro isomer also showed the upfield shift of the Pro-ring protons and a small coupling constant (4.5 Hz) between the Phe^2 Cα and amide protons. Taken together, these data strongly support a type VI β-turn structure for residues 1–4 as the major conformation present in solution. The strong NOE connectivity between the Ala^6 and the Phe^1 amide protons indicates a β turn structure for residues Trp^4 to Phe^1. Therefore, the *cis* Pro conformation consists of two interlocking β-turns.

The conformation and environment of the Pro ring in the *cis* Pro structure is well defined. The COSY spectrum (Fig. 5) showed a small coupling constant (<2 Hz) between the $C_\alpha H$ and the $C_{\beta 2}H$ (measured in the crosspeak between the $C_\alpha H$ (3.4 ppm) and the $C_{\beta 3}H$ (0.6 ppm)) and small coupling constants for the pairs of protons $C_\alpha H$ and $C_{\beta 2}H$, $C_{\beta 2}H$ and $C_{\gamma 3}H$, and $C_{\gamma 3}H$ and $C_{\delta 2}H$ (as indicated by a lack of these crosspeaks), consistent with a Cβ-*exo*/Cγ-*endo* Pro-ring pucker [16]. The *cis* Pro low-energy conformations generated by conformational search (Fig. 3a) all show this ring-pucker conformation and torsion angles for the pairs of protons close to 90°. The particularly strong upfield shifts of two protons, $C_{\gamma 2}H$ (0.3 ppm) and $C_{\beta 3}H$ (0.6 ppm) (Fig. 5), suggested that the Phe^2 and Trp^4 aromatic sidechains were near the Pro ring, as found for linear peptides with a Pro residue flanked by two aromatic residues [15,16]. The proximity of the Phe^2 and Trp^4 aromatic rings to Pro^3 was further shown by NOE connectivities, two of which could be definitively assigned: the first between the Pro Cα and Phe^2 Cδ protons and the second between the Pro Cδ2 and Trp Cδ1 protons. In addition, the Pro Cβ3 proton, which is close to the Cα proton, had an NOE connectivity with an aromatic proton at 7.3 ppm. This proton was likely to be one of the Phe^2 Cε or Cζ protons. These NOE connectivities are consistent with the low-energy *cis* Pro structures found by computational search, which have a Cβ-*exo*/Cγ-*endo* ring pucker that places Pro Cα and Cδ2 on opposite sides of the Pro ring and adjacent to the Phe^2 and Trp^4 sidechains, respectively (Fig. 3a).

The proton resonances of the *trans* Pro conformation were similar to those observed for linear peptides of closely related sequence [14]. In CD_3CN, an NOE connectivity between the Phe^2 Cα and the Pro Cδ protons could be unambiguously assigned, showing a *trans* peptide bond. An NOE connectivity between the Pro $C_\alpha H$ and the Trp^4 amide protons and the lack of an NOE connectivity between the Phe^2 Cδ and Trp^4 amide protons were consistent with a type II β-turn for residues Phe^2 to Gly^5. Crosspeaks in the COSY spectrum between the Pro $C_\alpha H$ (4.2 ppm) and the Cβ protons were less distinct than for the *cis* Pro conformation, suggesting a mixture of Pro-ring puckers, as seen in the low-energy *trans* Pro structures found by conformational search. Chemical shifts for the *trans* Pro-ring protons (Table 4) were similar to those found for the *trans* Pro conformation of the peptide Ser–Tyr–Pro–Tyr–Asp–Val [14]. A strong NOE connectivity between the Phe^1 and the Phe^2 amide protons indicated a β-turn structure for residues Gly^4 to Phe^2, so the *trans* Pro conformation, like the *cis* Pro structure, consisted of two interlocking β-turns.

Figure 5

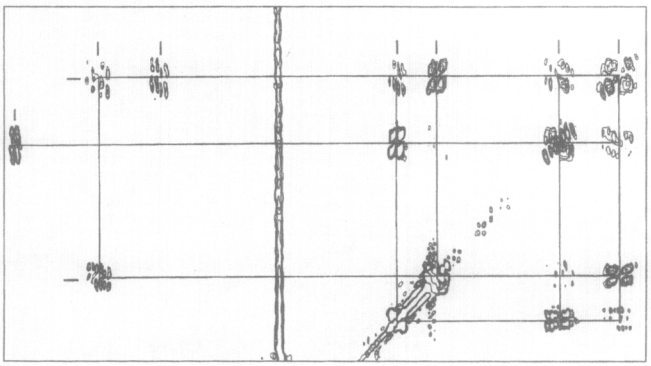

Portion of the 300 MHz COSY spectrum of cyclo-(APF[Phe^2,Ala^6]) showing the resonances of the Pro^3 ring protons in the *cis* Pro, type VI β-turn conformation.

Exchange crosspeaks between the *cis* and *trans* conformations, which had the opposite sign to the NOE connectivities, were present for all Pro protons, the amide protons of Phe^2, Trp^4 and Gly^5 and the β protons of Phe^2. The NMR spectra of closely related linear peptides do not display crosspeaks [15], indicating a more rapid rate of *cis–trans* isomerization for cyclo-(APF[Phe^2,Ala^6]). This rapid isomerization may have been due to the increased strain of the peptide bonds in the cyclized peptide [17]. The presence of CD_3CN in the sample may also have enhanced the isomerization rate. These exchange peaks provided an additional check of the proton assignments.

Discussion

Insect kinin active core optimized for β-turn of residues 1–4

The flexibility of linear peptides makes it difficult to determine the receptor-bound conformation, even for small

pentapeptides. Molecular dynamics simulations of four leucokinin active-core pentapeptides (position 2 = Tyr, Ser, Asn or His), however, revealed a preferred β-turn conformation for residues 1–4 (Fig. 1). This structure correlates with the importance of each active-core residue found by structure–activity data. In the β-turn conformation, the two essential sidechains, Phe^1 and Trp^4, are adjacent to each other and on the same side of the mainchain backbone. In contrast, the sidechain of residue 2, which tolerates a wide variety of substitutions [6] and shows natural variation, lies on the opposite side of the mainchain backbone, extending away from the surface formed by Phe^1 and Trp^4 (Fig. 1). The achetakinin active-core pentapeptide APF[Tyr^2] structure that has a *cis* peptide bond preceding Pro^3 (*cis* Pro) adopted a closely related conformation (Fig. 1).

Based on data for β-turn occurrence in proteins [12,13], the kinin active cores would be expected to have a greater β-turn preference for residues 2–5 than for residues 1–4. These data do not, however, take adjacent sidechains into account nor do they necessarily mirror β-turn preferences of small peptides in solution. In contrast, systematic NMR studies on linear pentapeptides with Pro^3 [15,16] demonstrate that aromatic sidechains that flank Pro promote *cis* Pro formation and enhance the percentage of type VI β-turns (*cis* Pro in the third position of the turn) within the *cis* Pro population [15]. A small, hydrophilic residue (Asp, Ser, Thr, Gly or Asn) following the aromatic–Pro–aromatic motif further promotes type VI β-turn formation [15]. In addition, our computational results on the insect kinins suggest that interactions between aromatic sidechains in positions 1 and 4 also promote β-turn formation for residues 1–4. Therefore, with aromatic residues at positions 1, 2 and 4 and Gly at position 5, the achetakinin active-core sequence pattern appears to be optimized for adopting a type VI β-turn in solution. In the leucokinin active core, the achetakinin *cis* Pro is replaced by Ser^3 that is preceded by a *trans* peptide bond. Despite this, the preferred leucokinin conformation, as indicated by molecular dynamics simulations, resembles that of the achetakinin active core in its relative sidechain orientations and the presence of a β-turn for residues 1–4. As for the Pro-containing peptides, favorable interactions of the adjacent aromatic sidechains with the position 3 (Ser) sidechain and backbone may promote this β-turn preference and would explain why leucokinin active-core peptides with Tyr^2 and Phe^2 are more active than those with Ser, Ala (Tables 1 and 2) or other sidechains at position 2 [6]. Similarity of this preferred β-turn conformation in solution to the receptor-bound conformation would reduce the entropy loss upon binding, resulting in enhanced peptide–receptor binding, thereby correlating conformational preference with biological activity.

Biologically active, designed analog cyclo-(APF[Phe^2,Ala^6])

Because of decreased conformational freedom, active cyclic-peptide analogs are more useful for defining the receptor-bound conformation than are linear peptides. The proximity of the amino terminus to the carboxyl terminus in the preferred conformations found for the insect kinin active cores suggested that cyclic analogs could retain activity. We selected an achetakinin analog (Pro^3) rather than a leucokinin analog (Ser^3) to further restrict conformational freedom. Significant diuretic activity in the linear achetakinin analogs with Ala either preceding or following the active core (APF[Ala^0,Phe^2] and APF[Phe^2,Ala^6]) indicated that modifications required for end-to-end cyclization could be tolerated. The cyclized hexapeptide achetakinin analog cyclo-(APF[Phe^2,Ala^6]) displayed significant activity in both the diuretic (Table 1, Fig. 4) and myotropic (Table 2) assays, as well as strong binding to the diuretic receptor (Table 3).

Computational exploration of the conformational space of cyclo-(APF[Phe^2,Ala^6]), starting from six initial conformations for both *cis* and *trans* Pro, indicated that the *cis* Pro structure should retain the β-turn conformation found for the linear achetakinin active core. After equilibration (requiring 10–50 ps), each structure maintained a single conformation during the remainder of the molecular dynamics simulation (total of 100 ps), even when that conformation had a high potential energy compared with the lowest-energy structure found. Thus, for these cyclic peptides, the generation of multiple starting structures followed by molecular dynamics was a much more effective conformational search technique than a single extended molecular dynamics simulation.

For the *cis* Pro conformation of cyclo-(APF[Phe^2,Ala^6]), the conformational search results agree with the NMR data and are consistent with previous NMR data on linear Pro-containing peptides [15,16]. The *in vacuo* search indicates that the *cis* Pro structure has a lower energy than the *trans* Pro structure, consistent with the 60:40 mixture of *cis*:*trans* Pro structures seen by NMR. Both the conformational search (Fig. 3a) and COSY (Fig. 5) and ROESY spectra supported a well-defined type VIA β-turn with a Cβ-*exo*/Cγ-*endo* pucker for the Pro ring as the predominant conformation. Therefore, our *in vacuo* conformational search, which included no constraints from the NMR data, successfully predicted the important structural features of the *cis* Pro conformation. The *trans* Pro conformation, however, showed significant structural variability by conformational search, displaying type I and type II turns of similar energy, whilst the ROESY spectra showed evidence only for a type II conformation.

The low-energy structures calculated for *cis* Pro cyclo-(APF[Phe^2,Ala^6]) share specific structural characteristics with those found for the linear active-core pentapeptides by molecular dynamics conformational search. The essential Phe^1 and Trp^4 sidechains lie adjacent to each other on one surface of the mainchain ring and the highly replaceable

position 2 sidechain lies on the opposite surface. Phe[1] and Trp[4], along with the mainchain atoms of residues 2 and 3, form a continuous, chemically conserved surface (Fig. 3a), which could be presented to a receptor molecule. The resemblance of the cyclo-(APF[Phe^2,Ala^6]) *cis* Pro structure to the shared conformation of the linear active cores and the consistency of the general sidechain orientation of the *cis* Pro structure with the Ala-substitution structure–activity data implicates the *cis* Pro backbone conformation in biological activity.

The low-energy *trans* Pro conformation of cyclo-(APF[Phe^2,Ala^6]) (Fig. 3b) appears to be less consistent with the current structure–activity data. The two essential aromatic sidechains are distant from each other on opposite sides of the cyclic peptide backbone. A related *trans* Pro structure has been found for a cyclic octapeptide analog of the leucopyrokinin neuropeptide family [18,19], which has the active core Phe–X–Pro–Arg–Leu (X = Ser, Thr or Val) ending in a carboxy-terminal amide [20]. In the leucopyrokinins, however, the residues flanking the Pro residue do not contain aromatic sidechains, which are the main determinants for *cis* Pro formation in linear peptides [14,15].

Receptor binding versus signal transduction

Because biological activity assays have components of both receptor binding and signal transduction, reduction of either component could decrease biological activity. Direct examination of diuretic receptor binding by displacement of a bound, radiolabeled ligand (Table 3) showed that modification of the carboxyl terminus had surprisingly little effect on receptor binding in contrast with the effects on biological activity. Although the dissociation constant of the carboxy-terminal acid APF[Ala^0,Phe^2]–OH was only twice that of the corresponding carboxy-terminal amide APF[Ala^0,Phe^2] (Table 3), the acid was 50000-fold less active (Table 1). Both APF[Ala^0,Phe^2] and its linear permuted analog APF[Phe^2,Ala^6] displayed similar receptor binding (Table 3), but APF[Phe^2,Ala^6] had a 20-fold reduction of diuretic activity. The tetrapeptide sequence Phe–Phe–Pro– Trp is shared in all three analogs, and therefore appears to be largely responsible for receptor binding. The carboxy-terminal region appears much less important for binding, but modulates activity, suggesting that it has a role in signal transduction. An important, conserved role in signal transduction may explain the requirement for a carboxy-terminal amide in many insect and mammalian neuropeptide families.

Modification of the carboxyl terminus may be the primary cause for the decreased activity of cyclo-(APF[Phe^2,Ala^6]) when compared with the highly active APF[Ala^0,Phe^2]. If the conformationally constrained cyclic analog fits the receptor-bound conformation of the linear analogs, it should display tighter receptor binding due to its decreased entropy loss relative to linear analogs. Indeed, cyclo-(APF[Phe^2,Ala^6]) displayed the tightest binding of the analogs tested (Table 3), indicating that its decreased activity is due to reduced signal transduction rather than decreased receptor binding. Models for signal transduction [21,22] suggest that it is caused by a conformational change in the receptor upon ligand binding. In the insect kinin neuropeptides, modification of the carboxy-terminal region may influence the ligand's ability to induce this conformational change. For the cyclic analog, reduced flexibility may also contribute to reduced signal transduction.

The myotropic activity profile for carboxy-terminal modified analogs parallels the diuretic activity profile: no activity with a carboxy-terminal carboxylate and decreased activity with addition of a residue at the carboxyl terminus. Therefore, as for diuretic activity, reduced myotropic activity in these analogs may reflect decreased signal transduction rather than decreased receptor binding. The similar Ala-substitution activity profiles suggest that closely related conformations for the insect kinin neuropeptides are required for both diuretic and myotropic activity. The greater sensitivity of myotropic activity to modifications at the carboxyl terminus indicates that selective antagonists could be designed to block one function over another; an important goal in regulating the actions of multifunctional neuropeptides.

Correlation between sequence, conformation and activity for the insect kinin neuropeptides

The consensus β-turn stereochemistry found by molecular dynamics simulations for the insect kinin pentapeptide active core is consistent with the structure–activity data obtained to date. In this conformation, the sidechains of residues Phe[1] and Trp[4] can be presented to the receptor as a continuous surface, consistent with their essential role in receptor binding. Positions 2 and 3 tolerate greater sidechain variation, consistent with their role as conformational determinants. The strong receptor binding of our designed, conformationally restrained cyclic analog indicates that residues 1–4 have the geometry required for recognition by the receptor molecule. Myotropic and diuretic activities have different sensitivities to changes of the carboxy-terminal residue, suggesting that modifications of this residue could be used to influence one activity over the other. The decreased activity of the cyclic analog and other carboxy-terminal modified analogs, despite strong receptor binding, implicates the amidated carboxyl terminus in signal transduction. Thus, our combined experimental and computational approach has characterized the active conformation, delineated specific roles for the active-core residues and provided a basis for the design of agonists and antagonists. This approach may prove useful for defining the structural chemistry for neuropeptide–receptor interactions of other neuropeptide families, such as the myotropic and hypotensive vertebrate

peptides, the tachykinins, which also share a common carboxy-terminal sequence (Phe–X–Gly–Leu– Met–NH_2, X=Tyr, Phe, Ile or Val) [23].

Significance

Biologically active peptides are often the starting compounds in attempts at drug design, but their flexibility makes it difficult to determine their bioactive conformation. A peptide may induce multiple functions, but the goal of the design is often to develop selective compounds that influence only one function. To address these concerns, we have applied a combined experimental and theoretical approach to the insect kinin neuropeptides in order to elucidate requirements for activity. The insect kinins have several advantages for this type of interdisciplinary study: their short carboxy-terminal pentapeptide (Phe^1–X^2–X^3–Trp^4–Gly^5–NH_2, X^3 = Ser or Pro) is fully active, facilitating analog synthesis and computational conformational search; preliminary sequence–activity information is provided by the many members of the insect kinin family; two distinct biological assays have been developed, one measuring muscle contractile (myotropic) activity and the other measuring diuretic activity; and finally, diuretic receptor binding can be examined directly, enabling receptor binding to be distinguished from signal transduction.

Analysis of our sidechain-replacement studies and the results of our computational conformational search on the highly active carboxy-terminal pentapeptide suggested that each sidechain has a discrete role in receptor recognition, conformational preference or the differentiation between myotropic and diuretic activities. This dissection of the carboxy-terminal pentapeptide will be valuable for directing future developments of compounds for insect control. The preferred β-turn conformation found for residues 1–4 by conformational search was retained in a designed, biologically active, conformationally constrained cyclic analog, as shown both by conformational search and NMR spectroscopy, demonstrating that *in vacuo* computational search can successfully predict solvated structure. Although many analogs containing carboxy-terminal residues 1–4 bound the diuretic receptor, the amidated carboxyl terminus was required for strong diuretic activity. Thus, the carboxy-terminal amide, required for activity in many insect and mammalian neuropeptide families, may have a general role in signal transduction. This role offers an intriguing basis for guiding the design of agonists over antagonists.

Materials and methods

Diuretic assay

Diuretic activity was determined in the Ramsey assay [24] with isolated Malpighian tubules from the house cricket, *Acheta domesticus*, as described elsewhere [25]. Briefly, single tubules were transferred to small (5 μl) drops of cricket saline beneath water-saturated liquid paraffin. The proximal end of each tubule was withdrawn from the saline and the secreted fluid escaped into the surrounding paraffin from a small cut made just distal to where the tubule was anchored into a block of Sylgard™. At intervals, the drops of secreted fluid were displaced from the tubules and their volume, and hence the rate of secretion, was obtained by measuring the diameter of the drops, assuming them to be perfect spheres. After a 40 min equilibration period, rates of secretion were determined over 40 min intervals before and after the addition of test compounds to the saline bathing the tubules. Results, in picoliters per millimeter tubule length per min (pl mm^{-1} min^{-1}) are expressed as a percentage of the response to a supramaximal dose (50 nM) of achetakinin-I assayed alongside the test substances. Dose-response curves were fitted to the generalized logistic equation using the curve-fitting program FigP (Biosoft, Cambridge, UK).

Myotropic assay

Hindguts from *Leucophaea maderae* cockroaches were dissected, suspended in a 5 ml muscle chamber, and prepared for recording as previously described [26]. Threshold concentrations were determined for each peptide by adding a known quantity of peptide (dissolved in 0.5 ml bioassay saline) to the bioassay chamber containing the hindgut. The quantity of peptide was calculated from the values obtained for Phe or Gly in the amino acid analysis. The threshold concentration was defined as the minimum concentration of peptide required to evoke an observable change in the frequency (50%) or amplitude (10%) of contractions within 1 min and sustained for 3 min. Threshold concentrations were obtained from five cockroach hindguts on five consecutive days for each peptide.

Diuretic receptor-binding assay

The affinities of achetakinin analogs for receptors on Malpighian tubule plasma membranes were determined in competition assays using an ^{125}I-labeled analog of achetakinin-II (3′hydroxyphenyl propionic-Gly–Gly–Gly–Phe–Ser–Pro–Trp–Gly–NH_2), specific activity >1100 Ci mM^{-1}, as the radioligand [27]. Malpighian tubules were transferred to a dissection buffer (25 mM Tris-maleate, 0.6 mM EGTA, pH 7.4) containing a cocktail of protease inhibitors [27] and were disrupted using a Polytron™. After centrifugation for 10 min at 1000 g (4°C), the supernatant was subjected to a further 30 min of centrifugation at 30 000 g (4°C). The resulting pellet was resuspended in dissection buffer and the high-speed centrifugation was repeated. The protein content in the resulting membrane pellet was determined by the method of Bradford [28].

An incubation buffer containing 25 mM Tris-maleate, 5 mM $MgCl_2$, 0.6 mM EGTA, 1% bovine serum albumin, and a cocktail of protease inhibitors at pH 7.4 [27] was used for the binding assay. Malpighian tubule membranes (100 μg membrane protein per 100 μl buffer) were incubated at room temperature for 60 min with the radioligand (50 000 cpm per assay tube) and different concentrations of test compounds. Nonspecific binding, measured in the presence of a 1000-fold excess of the unlabeled achetakinin-II analog, was subtracted from total binding to obtain specific binding. The concentration of a test compound that inhibited radioligand binding by 50% (IC_{50}) was determined from the generalized logistic equation with the computer program FigP.

Peptide synthesis

Peptides were synthesized [29–31], purified by HPLC [20] on a Waters μ-Bondapak phenyl or a C18 Radialpak liquid chromatography cartridge (Waters Assoc., Milford, MA, USA), and determined [29] to have the expected amino acid analyses. The cyclized achetakinin peptide fragment cyclo[Phe–Phe–Pro–Trp–Gly–Ala] (cyclo-(APF[Phe^2, Ala^6])) was synthesized by Donzel's procedure [32]. The leucokinin peptide fragments (LPF) and achetakinin peptide fragments (APF) showed the following amino acid analysis and retention times (RT in min) on a μ-Bondapak phenyl HPLC column: LPF[Tyr^2] [10] – F(1.0), G(1.2), S(1.0), Y(1.0), RT=27.4; LPF[Phe^2] [10] – F(2.0), G(1.2), S(1.0), RT=33.7; LPF[Ser^2] [10] – F(1.0), G(1.0), S(1.9), RT=18.7; LPF[Ala^1,Tyr^2] – A(1.0), G(1.0), S(0.9), Y(1.1), RT = 16.6; LPF[Ala^2] – A(1.0), F(1.0), G(1.0), S(0.9), RT = 20.0; LPF[Tyr^2,Ala^3] – A(1.1), F(1.0), G(1.1), Y(1.0), RT = 28.2; LPF[Tyr^2,Ala^4] – A(1.0), F(1.0), G(1.1), S(1.0), Y(1.0), RT = 6.8;

LPF[Tyr^2,Ala^5] – A(1.0), F(1.0), S(0.9), Y(1.0), RT=28.2; LPF[dAla^2] – A(1.0), F(1.0), G(1.0), S(0.9), RT=25.2. Amino acid analysis and retention times (RT in min) on a C18 HPLC column were: LPF[Phe^2,Asn^5] – N(0.9), F(2.0), S(1.1), RT=20.0; LPF[Phe^2,Leu^5] – F(2.0), L(0.9), S(1.1), RT=25.0; APF[Phe^2,Ala^6] – OH–A(1.1), F(2.0), G(1.0), P(0.8), RT=26.5; LPF[Ala^0,Phe^2] – A(1.0), F(2.0), G(1.1), S(0.9), RT=29.2; APF[Ala^0,Phe^2] – A(1.0), F(2.0), G(1.0), P(0.9), RT=30.2; APF[Phe^2,Ala^6] – A(1.0), F(2.0), G(1.1), P(1.0), RT=34.2; cyclo-(APF[Phe^2,Ala^6]) – A(1.0), F(2.0), G(1.2), P(1.1), RT=37.2; cyclo-(LPF[Cys^0,Tyr^2,Cys^5]) – F(1.0), C(0.6), S(0.8), Y(0.9), RT=34.3. Amino acid analysis: APF[Phe^2] – F(2.0), G(0.8), P(0.9); APF[Ser^2]–F(1.0), G(1.0), P(0.9), S(0.9). Fast atom bombardment mass spectra were obtained according to previously described procedures [29,33]. Calc'd. for LPF[Cys^0,Tyr^2,Cys^5] (MH^+): 807.29; found: 807.10. Calc'd. for cyclo-(LPF[Cys^0,Tyr^2,Cys^5]) (MH^+): 805.27; found: 805.04. Mass spectra demonstrated that the parent MH^+ ion for cyclo-(APF[Phe^2,Ala^6]) was 18 mass units less than the linear precursor. Calc'd. for cyclo-(APF[Phe^2,Ala^6]) (MH+): 705.34; found: 705.40. cyclo-(APF[Phe^2,Ala^6]) showed no ninhydrin response, indicating there is no free amino-terminal amino group.

Conformational search with distance geometry and molecular dynamics techniques

Extended conformations of linear peptides were built, energy minimized, and subjected to molecular dynamics on Convex and Cray XMP supercomputers with the programs DISCOVER and INSIGHT (MSI, San Diego, USA) using the force field described by Dauber-Osguthorpe *et al.* [34]. Molecular dynamics were computed in time increments of 0.001 ps with a Verlet 'leap-frog' algorithm [35]. Template forcing was used to adjust the conformation of one peptide to that of another. In template forcing, a distance-dependent harmonic potential that forces specified atoms of one structure onto specified atoms of a second structure is added to the energy equation [36].

Cyclo-(APF[Phe^2,Ala^6]) was built with the peptide bond preceding the Pro in both *trans* and *cis* conformations with computer graphics using the graphics program INSIGHT. The *trans* Pro structure was based on the β-turn conformation found for leucopyrokinin [18]. The *cis* Pro structure was based on the β-turn conformation found for APF[Tyr^2] after template forcing to the β-turn conformation found for LPF[Tyr^2]. In addition, over 20 conformations of cyclo-(APF[Phe^2,Ala^6]) for both *cis* and *trans* Pro were generated by the program DGEOM, program 590 available from the Quantum Chemistry Program Exchange. Distance constraints were used to ensure proper bond lengths and valence angles, to fix the peptide bond geometry preceding Pro^3, and to close the mainchain ring. From these generated structures, five starting structures for both *cis* and *trans* Pro were selected based on reasonable peptide bond geometries and Cα stereochemistry. All 12 initial structures were energy minimized and then subjected to 100 ps of molecular dynamics, with snapshots taken every 10 ps. Dynamics simulations were viewed and analyzed with INSIGHT. Snapshots were energy minimized and analyzed visually, by calculation of the rms deviation of Cα atoms and by relative energetics. Figures 1, 2 and 3 were rendered with the AVS graphics program [37].

NMR spectroscopy

COSY, TOCSY and ROESY spectra of cyclo-(APF[Phe^2,Ala^6]) were acquired as previously described [14]. The sample for NMR was approximately 5 mM peptide, dissolved in 30% CD_3CN/70% H_2O (a mixture of 90% H_2O/10% D_2O), and adjusted to pH 4.2 at 20°C with 0.5 μl volumes of a 0.1 M NaOH solution. The 30% CD_3CN was required to dissolve the cyclic peptide. Spectra were repeated in 100% CD_3CN. Dioxan (chemical shift of 3.75 ppm) was added as the internal standard. Spectra were acquired on Bruker 300 and 500 MHz spectrometers. Data were processed on a Sun workstation with FELIX software (MSI, San Diego, USA).

Acknowledgements

We thank J. Yao, H. J. Dyson, G.P. Gippert, and R. Brueschweiler for generous assistance with the NMR spectra. We thank W. Haddon for mass spectra and J. Hicks for support of part of this work. Molecular dynamics were done at the San Diego Supercomputer Center and The Scripps Research Institute. The work was funded in part by PPG Industries, Inc., Pittsburgh, PA (R.J.N. and V.A.R.) and by grants from the National Science Foundation (BIR 92-23760 to J.A.T. and V.A.R.), from BBSRC (J.S.C.), and from NATO (910248 to R.J.N., G.M.C. and G.M.H.).

References

1. Lord, J.A.H., Waterfield, A.A., Hughes, J. & Kosterlitz, H.W. (1977). Endogenous opioid peptides: multiple agonists and receptors. *Nature* **267**, 495–499.
2. Laufer, R., Gilon, C., Chorev, M. & Selinger, Z. (1986). Characterization of a neurokinin B receptor site in rat brain using a highly selective radioligand. *J. Biol. Chem.* **261**, 10257–10263.
3. Hruby, V.J., Yamamura, H.I. & Porreca, F. (1995). Molecular organization of receptors: efficacy, agonists, and antagonists. *Ann. N.Y. Acad. Sci.* **757**, 7–22.
4. Hruby, V.J., Al-Obeidi, F. & Kazmierski, W. (1990). Emerging approaches in the molecular design of receptor-selective peptide ligands: conformational, topographical and dynamics considerations. *Biochem. J.* **268**, 249–262.
5. Holman, G.M., Nachman, R.J. & Wright, M.S. (1990). Comparative aspects of insect myotropic peptides. *Prog. Comp. Endocrinol.* **342**, 35–39.
6. Nachman, R.J. & Holman, G.M. (1991). Myotropic insect neuropeptide families from the cockroach *Leucophaea maderaea*: structure-activity relationships. In *Insect Neuropeptides: Chemistry, Biology and Action.* (Menn, J.J., Kelly, T.J. & Masler, E.P., eds) pp. 194–214, American Chemical Society, Washington DC, USA.
7. Schoofs, L., Holman, G.M., Proost, P., Van Damme, J., Hayes, T.K. & DeLoof, A. (1992). Locustakinin, a novel myotropic peptide from *Locusta migratoria*, isolation, primary structure and synthesis. *Regul. Pept.* **37**, 49–57.
8. Hayes, T.K., *et al.*, & Beyenbach, K.N. (1994). Culekinin depolarizing peptide: a mosquito leucokinin-like peptide that influences insect Malpighian tubule ion transport. *Regul. Pept.* **52**, 235–248.
9. Veenstra, J.A. (1994). Isolation and identification of three leucokinins from the mosquito *Aedes aegypti*. *Biochem. Biophys. Res. Commun.* **202**, 715–719.
10. Coast, G.M., Holman, G.M. & Nachman, R.J. (1990). The diuretic activity of a series of cephalomyotropic neuropeptides, the achetakinins, on isolated Malpighian tubules of the house cricket, *Acheta domesticus*. *J. Insect Physiol.* **36**, 481–488.
11. Hayes, T.K., *et al.*, & Beyenbach, K.W. (1989). Leucokinins, a new family of ion transport stimulators and inhibitors in insect Malpighian tubules. *Life Sci.* **44**, 1259–1266.
12. Chou, P.Y. & Fasman, G.D. (1977). β-Turns in proteins. *J. Mol. Biol.* **115**, 135–176.
13. Hutchinson, E.G. & Thornton, J.M. (1994). A revised set of potentials for β-turn formation in proteins. *Protein Sci.* **3**, 2207–2216.
14. Dyson, H.J., Rance, M., Houghten, R.A., Lerner, R.A. & Wright, P.E. (1988). Folding of immunogenic peptide fragments of proteins in water solution. *J. Mol. Biol.* **201**, 161–200.
15. Yao, J., Feher, V.A., Espejo, B.F., Reymond, M.T., Wright, P.E. & Dyson, H.J. (1994). Stabilization of a type VI turn in a family of linear peptides in water solution. *J. Mol. Biol.* **243**, 736–753.
16. Yao, J., Dyson, H.J. & Wright, P.E. (1994). Three-dimensional structure of a type VI turn in a linear peptide in water solution. *J. Mol. Biol.* **243**, 754–766.
17. Grathwohl, C. & Wuthrich, K. (1981). NMR studies of the rates of proline *cis-trans* isomerization in oligopeptides. *Biopolymers* **20**, 2623–2633.
18. Nachman, R.J., Roberts, V.A., Dyson, H.J., Holman, G.M. & Tainer, J.A. (1991). Active conformation of an insect neuropeptide family. *Proc. Natl Acad. Sci. USA* **88**, 4518–4522.
19. Nachman, R.J., Kuniyoshi, H., Roberts, V.A., Holman, G.M. & Suzuki, A. (1993). Active conformation of the pyrokinin/PBAN neuropeptide family for pheromone biosynthesis in the silkmoth *Bombyx mori*. *Biochem. Biophys. Res. Commun.* **193**, 661–666.
20. Nachman, R.J., Holman, G.M. & Cook, B.J. (1986). Active fragments and analogs of the insect neuropeptide leucopyrokinin: structure-function studies. *Biochem. Biophys. Res. Commun.* **137**, 936–942.
21. Stoddard, B.L., Biemann, H-P. & Koshland, D.E.Jr. (1992). Receptors and transmembrane signaling. *Cold Spring Harbor Symp. Quant. Biol.* **57**, 1–15.
22. Danielson, M.A., Biemann, H-P., Koshland, D.E., Jr & Falke, J.J. (1994). Attractant- and disulfide-induced conformational changes in the ligand binding domain of the chemotaxis aspartate receptor: a ^{19}F NMR study. *Biochemistry* **33**, 6100–6109.

23. Erspamer, V. (1981). The tachykinin peptide family. *Trends in Neurosci.* **4**, 267–269.
24. Ramsay, J.A. (1954). Active transport of water by the Malpighian tubules of the stick insect, *Dixippus morosus* (Orthoptera, Phasmidae). *J. Exp. Biol.* **31**, 104–113.
25. Coast, G.M. & Kay, I. (1994). The effects of *Acheta* diuretic peptide on isolated Malpighian tubules from the house cricket, *Acheta domesticus. J. Exp. Biol.* **187**, 225–243.
26. Holman, G.M., Nachman, R.J., Wright, M.S., Schoofs, L. & DeLoof, A. (1991). Insect myotropic peptides: isolation, structural characterization and biological properties. In *Insect Neuropeptides: Chemistry, Biology and Action.* (Menn, J.J., Kelly, T.J. & Masler, E.P., eds) pp. 40–50, American Chemical Society, Washington DC, USA.
27. Chung, J.S., Wheeler, C.H., Goldsworthy, G.J. & Coast, G.M. (1995). Properties of achetakinin binding sites on Malpighian tubule membranes from the house cricket, *Acheta domesticus. Peptides* **16**, 375–382.
28. Bradford, M.M. (1976). A rapid and sensitive method for the quantification of microgram quantities of protein utilizing the principle of protein-dye binding. *Anal. Biochem.* **72**, 248–254.
29. Nachman, R.J., Holman, G.M., Haddon, W.F. & Ling, N. (1986). Leucosulfakinin, a sulfated insect neuropeptide with homology to gastrin and cholecystokinin. *Science* **234**, 71–73.
30. Moroder, L. & Wunsch, E. (1986). Synthesis of cystine-peptides. In *New Trends In Natural Products Chemistry 1986, Studies In Organic Chemistry.* (Rahman, A. & Lequesne, P.W., eds) pp. 325–338, Elsevier, Amsterdam.
31. Spatola, A.F., Anwer, M.K., Rockwell, A.L. & Gierasch, L.M. (1986). Compatibility of β- and γ-turn features with a peptide backbone modification: synthesis and conformational analysis of a model cyclic pseudopentapeptide. *J. Amer. Chem. Soc.* **108**, 825–831.
32. Donzel, B., Rivier, J. & Goodman, M. (1977). Synthesis of a cyclic analog of the luteinizing hormone releasing factor: [Glu^4,D-Ala^6,Orn^7]LRF. *Biopolymers* **16**, 2587–2590.
33. Haddon, W., Handa, M., Lundin, R. & Nachman, R. (1987). Small computer-data system for research applications in mass spectrometry. In *Proceedings, 35th Conference on Mass Spectrometry and Allied Topics.* pp. 359–360, American Society of Mass Spectrometry, Denver, USA.
34. Dauber-Osguthorpe, P., Roberts, V.A., Osguthorpe, D.J., Wolff, J., Genest, M. & Hagler, A.T. (1988). Structure and energetics of ligand binding to proteins: *Escherichia coli* dihydrofolate reductase-trimethoprim, a drug-receptor system. *Proteins* **4**, 31–47.
35. Hockney R.W. & Eastwood J.W. (1981) Computer Simulations of Particles. McGraw-Hill, New York, USA.
36. Struthers, R.S., Rivier, J. & Hagler, A.T. (1985). Molecular dynamics and minimum energy conformations of GnRH and analogs. *Ann. N.Y. Acad. Sci.* **439**, 81–96.
37. Upson, C., *et al.*, & van Dam, A. (1989). The application visualization system: a computational environment for scientific visualization. *IEEE Comp. Graph. Appl.* **9**, 30–42.